$Co_3O_4/Fe_{0.33}Co_{0.66}P$ Interface Nanowire for Enhancing Water Oxidation Catalysis at High Current Density

Xiaoyan Zhang, Jing Li, Yong Yang, Shan Zhang, Haishuang Zhu, Xiaoqing Zhu, Huanhuan Xing, Yelong Zhang, Bolong Huang*, Shaojun Guo* and Erkang Wang*

Mrs. X. Zhang, Prof. J. Li, Ms. S. Zhang, Ms. H. Zhu, Ms. X. Zhu, Ms. H. Xing, Prof. E. Wang
State Key Laboratory of Electroanalytical Chemistry, Changchun Institute of Applied Chemistry, Chinese Academy of Sciences, Changchun, Jilin 130022, China
University of Chinese Academy of Sciences, Beijing, 100049, China

Mrs. X. Zhang, Dr. Y. Yang, Ms. S. Zhang, Dr. Y. Zhang, Prof. S. Guo
Department of Materials Science & Engineering, College of Engineering, Peking University, Beijing 100871, China

Prof. S. Guo
BIC-ESAT, College of Engineering, Peking University, Beijing 100871, China.

Prof. B. Huang
Department of Applied Biology and Chemical Technology, The Hong Kong Polytechnic University, Hung Hom, Kowloon, Hong Kong SAR, China

E-mail: lijingce@ciac.ac.cn; bhuang@polyu.edu.hk; guosj@pku.edu.cn

Keywords: nanowire; semi-metallic interface; oxygen evolution reaction; electrocatalysis

Abstract

Designing the well-defined nanointerface is of prime importance to enhance the activity of nanoelectrocatalysts for different catalytic reactions. However, studies on non-noble metal interface electrocatalysts with extremely high activity and superior stability at high current density still remains a great challenge. Herein, we rationally design a class of $Co_3O_4/Fe_{0.33}Co_{0.66}P$ interface nanowire for boosting oxygen evolution reaction (OER) catalysis at high current density by partially

chemical etching of $Co(CO_3)_{0.5}(OH)\cdot 0.11H_2O$ (Co-CHH) nanowire with $Fe(CN)_6^{3-}$, followed by low temperature phosphorization treatment. The resulting $Co_3O_4/Fe_{0.33}Co_{0.66}P$ interface nanowire exhibits very high OER catalytic performance with the overpotential of only 170 mV at the current density of 20 mA cm^{-2} and Tafel slope of 59.8 mV dec^{-1} in 1.0 M KOH. In particular, the $Co_3O_4/Fe_{0.33}Co_{0.66}P$ exhibits an obvious advantage in enhancing oxygen evolution at high current density by showing the overpotential of merely 291 mV at 800 mA cm^{-2}, much lower than that of RuO_2 (446 mV). The $Co_3O_4/Fe_{0.33}Co_{0.66}P$ is remarkably stable for OER with negligible current loss under the overpotentials of 200 mV and 240 mV for 150 h. Theoretical calculations unveil that $Co_3O_4/Fe_{0.33}Co_{0.66}P$ is more favorable for OER since the electrochemical catalytic oxygen evolution barrier was optimally lowered down by the active Co and O sites from the $Co_3O_4/Fe_{0.33}Co_{0.66}P$ interface. This work not only presents a controllable interface-engineering method for the design of $Co_3O_4/Fe_{0.33}Co_{0.66}P$ interface nanowire as a robust OER electrocatalyst but also provides an insight into the relationship between $Co_3O_4/Fe_{0.33}Co_{0.66}P$ interface and OER catalytic performance.

Introduction

Oxygen evolution reaction (OER, $4OH \rightarrow O_2 + 2H_2O$) plays an important role in renewable energy conversion processes such as water splitting, metal-air batteries and CO_2 reduction[1-4]. However, its sluggish kinetics greatly limits its practical application[5-7]. In this regard, excavating a suitable electrocatalyst, which can overcome the activation energy to break O-H bond and form O-O double bond, is highly desirable but still remains a great challenge[8]. Among state-of-the-art electrocatalysts, the oxides of iridium (IrO_2) and ruthenium (RuO_2) have been known as the best OER electrocatalysts[9]. However, the scarcity, high cost and inferior stability have suppressed their upscale development[10-12]. Seeking for earth-abundant and high efficient OER catalysts to replace noble metals has been placing on the agenda.

First-row transition metals have been extensively studied for OER catalysis on account of their splendid performance and abundant resources[13-14]. In particular, cobalt (Co)-based compounds such as oxides[15], borides[16], sulfides[17], selenides[18], phosphides[19] and so on have been rapidly developed. Among them, Co_3O_4 is a promising OER electrocatalyst in alkaline environment but the application of bulk Co_3O_4 is hampered by its poor conductivity and low surface area[20-22]. Considerable efforts have been devoted to boosting OER performance of Co_3O_4 through growing nanosized Co_3O_4 onto conductive substrate (*e.g.* carbon nanotube[23] and reduced graphene oxide[24]), doping heteroatoms (*e.g.* Fe[25], Ni[26], Zn[27], N[28], P[22]) into Co_3O_4 to modify its electronic properties, and hybridizing Co_3O_4 with other compounds[29-30] to tune its catalytic properties. Creating nanointerface (*e.g.* NiO/CoN[31], NiS_2/CoS_2[32], CuS/NiS_2[33] and Co/Co_2C[34]) has been recently regarded as an effective way to enhance the activity of electrocatalyst. The charge transfer rate can be increased due to the interaction between different components at the interface[33]. However, it is still a great challenge to synthesize Co_3O_4-based interfacial nanomaterials with glorious performance for OER. Here, we report a novel one-dimensional $Co_3O_4/Fe_{0.33}Co_{0.66}P$ interface nanowire on nickel foam (NF) *via* partially chemical etching of $Co(CO_3)_{0.5}(OH)\cdot 0.11H_2O$-cobalt carbonate hydroxide hydrate (Co-CHH) nanowire by $Fe(CN)_6^{3-}$ to create Co-CHH/$FeCo_2(CN)_6$ interface followed by phosphorization treatment at low temperature. The as-made $Co_3O_4/Fe_{0.33}Co_{0.66}P$ interface nanowire exhibits excellent OER performance in 1.0 M KOH by showing the overpotential of only 170 mV at the current density of 20 mA cm^{-2} and the Tafel slope of 59.8 mV dec^{-1}. Density functional theory (DFT) calculations are used to explore the catalytic mechanism, which predicts that the electrochemical catalytic barrier was optimally lowered down by the active Co and O sites from the $Co_3O_4/Fe_{0.33}Co_{0.66}P$ interface. Particularly, the $Co_3O_4/Fe_{0.33}Co_{0.66}P$ interface nanowire exhibits superior OER performance at high current density due to the actualization of high efficient charge spatial separation with electron-hole rich agglomerated region within the interface proved by DFT calculations. The overpotentials were only 239, 257 and 291 mV when the current densities reached 300, 500 and 800 mA cm^{-2},

respectively. Moreover, the durability of $Co_3O_4/Fe_{0.33}Co_{0.66}P$ was also decent even after 150 h under the overpotentials of 200 mV and 240 mV. The unprecedented OER performance manifested the importance of interface engineering in designing OER electrocatalyst.

Results and Discussions

The construction of $Co_3O_4/Fe_{0.33}Co_{0.66}P$ interface nanowire was depicted in **Figure 1a**. In brief, $Co_3O_4/Fe_{0.33}Co_{0.66}P$ interface nanowire was made by partially etching $Co(CO_3)_{0.5}(OH)\cdot 0.11H_2O$-cobalt carbonate hydroxide hydrate (Co-CHH) nanowire **(Figure 1b and Figure S1)** with $Fe(CN)_6^{3-}$ to form the precursor Co-CHH/$FeCo_2(CN)_6$ **(Figure 1c and Figure S2)**, followed by phosphorization with $NaH_2PO_2\cdot H_2O$ under 350 °C. The second hydrothermal reaction time is of prime importance for the generation of $Co_3O_4/Fe_{0.33}Co_{0.66}P$ interface. Too short reaction time (3 h) or too long reaction time (18 h) would lead to completely unetching and etching of Co-CHH nanowire. Their further phosphorization resulted in the formation of Co_3O_4/FeP **(Figure S3)** and $Fe_{0.33}Co_{0.66}P$ **(Figure S4)**, respectively.

The scanning electron microscopy (SEM) **(Figure 1d)** and transmission electron microscopy (TEM) images **(Figure 1e)** of $Co_3O_4/Fe_{0.33}Co_{0.66}P$ interface nanowire show the formation of heterostructure with nanoparticles anchored onto nanowire skeleton. Its X-ray diffraction (XRD) pattern is in accordance with those of Co_3O_4 (JCPDS NO. 65-3103) and CoP (JCPDS NO. 29-0497) **(Figure S5a)**, belonging to the space groups of $Fd\bar{3}m$ (a = b = c = 8.056 Å) with cubic structure and Pnma (a = 5.077 Å, b = 3.281 Å, c = 5.587 Å) with orthorhombic structure, respectively. The partial replacement of Co atoms with Fe atoms did not give rise to the change of CoP crystal structure. Elemental mapping **(*inset* in Figure 1e)** shows that Co, Fe and P elements are uniformly dispersed along the $Co_3O_4/Fe_{0.33}Co_{0.66}P$ interface nanowire. The energy dispersive X-ray (EDX) result, the combination of ICP and XPS **(Figure S5b and Table S1)** both demonstrate the successful formation of $Co_3O_4/Fe_{0.33}Co_{0.66}P$**.** High-resolution TEM (HRTEM) image in **Figure 1f** shows two

lattice fringe spacings of 1.86 Å and 2.83 Å, corresponding to (331) plane of cubic Co_3O_4 and (011) plane of orthorhombic $Fe_{0.33}Co_{0.66}P$, respectively. This result further verifies the successful construction of Co_3O_4 and $Fe_{0.33}Co_{0.66}P$ heterojunction interface.

X-ray photoelectron spectroscopy (XPS) was used to characterize the composition and valence states of $Co_3O_4/Fe_{0.33}Co_{0.66}P$ interface nanowire. **Figure S6a** shows the signals of Co, Fe, P and O, being in accordance with EDX result. The binding energy of Co $2p_{3/2}$ at 778.9 eV is positively shifted by 0.8 eV compared with that of pure CoP **(Figure S6b)** while the Fe $2p_{3/2}$ peak at 707.2 eV is negatively shifted by 0.3 eV with respect to that of pure FeP **(Figure S6c)**. This phenomenon could be ascribed to the electron donation from Co to Fe[35]. In P 2p spectrum, the electron binding energies of 128.7 eV and 129.6 eV are ascribed to P $2p_{3/2}$ and P $2p_{1/2}$, respectively **(Figure S6d)**, the downshift of which with respect to pure P element suggests the formation of phosphide as well as the strong electron interaction of Co/Fe and P[36].

Distinguished catalytic performance of water oxidation performance by Co_3O_4 and CoP has been greatly reported from literatures[37-46]. However, the role of interface has not yet been fully excavated. Accordingly, we have built the interface (IF) model of $Co_3O_4/Fe_{0.33}Co_{0.66}P$ system for a deep exploration of the electrocatalytic OER activity (**Figure 2**). It has been extensively studied that the interplaying conversion between Co^{II} and Co^{III} determines the reactivity of the water oxidation from Co_3O_4[37]. Note that, the Co^{II} species present in the spinel structure of Co_3O_4 usually easily transform into the Co^{III} that constrains the reactivity with less distinguishable overpotential to RuO_2. This is due to the Co-3d-band from the Co_3O_4 potentially exhibits the over-binding effect to the adsorbing species as the center is greatly close to the E_F. From our calculation, we reasoned that this effect has been alleviated by the $Fe_{0.33}Co_{0.66}P$ with assistance of Fe-dopant. Moreover, here we emphasize the interfacial modulating effect on the Co-3d-band states with influence of $Fe_{0.33}Co_{0.66}P$ component.

For this purpose, structural configuration is necessary to be prepared, in which the Fe substituted one third of Co site of the CoP as $Fe_{0.33}Co_{0.66}P$ layer and the Co_3O_4 layer is directly truncated from the spinel bulk lattice **(Figure 2a)**. From that, the Co/IF and Fe/IF represent the Co and Fe sites from IF region respectively. The Co/Co_3O_4 and $Co/Fe_{0.33}Co_{0.66}P$ are the Co-sites from the internal lattice of the Co_3O_4 and $Fe_{0.33}Co_{0.66}P$ respectively. Actually, the Co/IF still maintains high coordination number (CN) surrounded by P and O sites. The valence states Co and Fe sites are different according to their different local bonding environment. Contour plots of the valence orbital confirm that the vicinity of IF region is mainly the electron-hole-rich area **(Figure 2b)**, where represents the occupied (HOMO) and empty (LUMO) states near the Fermi level (E_F). The analysis of the projected density of states (PDOSs) clearly exhibits the tuning trend of the interfacial electronic properties. We see that, the Co-3d-band at the IF downshifts further to a level slightly deeper than the one found in $Fe_{0.33}Co_{0.66}P$. This shift not only provides higher rates of electron-rich Co-site (Co^{II}) but also forms an electronic barrier for inhibiting oxidation backward (Co^{III}). The PDOSs analysis also supports that the Co-site at the IF region can effectively proceed the electron-proton charge exchange with a fast adsorption and desorption process **(Figure 2c)**. We also notice that the Fe-3d-band stays in the intermediate range, showing its significant relay-band-center role in continuously tuning the electronic properties gradually towards an optimal performance *via* on-site orbital Coulomb potential effect **(Figure 2c)**. The orbital activities of Fe- and Co-sites under different local bonding environment have been further analyzed and compared (Figure S16) based on our recently developed *ab*-initio method[47-48].

Moving onto the *p-d* orbital overlapping effect, we found both roles of P and O sites within the IF system are irreplaceable. Based on the PDOSs results, four different sites (Fe, Co, O, and P) near the IF region shows their electronic active p- and d- orbitals respectively. The deep localized P-3p-band within the system can restrain the surface oxidation rates and hence to minimize over-binding effect between P-site and O-related species. By the on-site Coulomb *p-d* repulsion, the high lying O-

2p-band (closer to the E_F) guarantees the certain electronic activities for overlapping the H-1s orbital and stabilizes the intermediate H-adsorbates **(Figure 2d)**. Moreover, as we compare, only the Co-3d and O-2p could perform a good band overlapping, which confirms the determining role of the reactivity by the Co-site. Our analysis shows water splitting effect and locating the intermediates can be simultaneously accomplished by the Co and O sites near the IF **(*inset* in Figure 2d)**.

The OER activities of different catalysts were evaluated in O_2-saturated 1.0 M KOH **(Figure 3a)**. As expected, RuO_2 on NF exhibits excellent OER performance with the overpotential of 204 mV reaching the current density of 20 mA cm^{-2}. Surprisingly, the OER activity of $Co_3O_4/Fe_{0.33}Co_{0.66}P$ interface nanowire was superior to RuO_2. To reach the current density of 20 mA cm^{-2}, $Co_3O_4/Fe_{0.33}Co_{0.66}P$ on NF only needs the overpotential of 170 mV, 34 mV smaller than that of RuO_2 on NF. Note that the oxidation peak at 1.36 V is assigned to Ni^{2+} to Ni^{3+}, which is reversible[49], demonstrated by cyclic voltammetry (CV) curve in **Figure S7**. Such overpotential is also 164, 163 and 206 mV less than those of Co-CHH/$FeCo_2(CN)_6$, Co-CHH on NF and bare NF.

In particular, the as-prepared $Co_3O_4/Fe_{0.33}Co_{0.66}P$ interface nanowire shows outstanding OER performance at high current density, rarely achieved in previous researches **(Figure 3b and Table S2)**. With increasing the current density, the increment of corresponding overpotential for $Co_3O_4/Fe_{0.33}Co_{0.66}P$ is surprisingly small. Even the current density reaches 800 mA cm^{-2}, the overpotential is still less than 300 mV. However, RuO_2 on NF needs the overpotential of 446 mV to reach the current density of 800 mA cm^{-2}, 155 mV larger than that of $Co_3O_4/Fe_{0.33}Co_{0.66}P$ on NF, indicating the great advantage of $Co_3O_4/Fe_{0.33}Co_{0.66}P$ at high current density. We also catch the moment of $Co_3O_4/Fe_{0.33}Co_{0.66}P$ and RuO_2 on NF at the current density of 800 mA cm^{-2}. It can be obviously observed that uniform gas bubbles escaped immediately from the surface of $Co_3O_4/Fe_{0.33}Co_{0.66}P$ with almost no catalyst peeled off **(Figure S8a)**, demonstrating its splendid aerophobic feature and the intimate contact between the electrocatalyst and substrate. On the contrary, the bubbles accumulated on RuO_2 surface are hard to diffuse, and there are a lot of catalysts

falling off **(Figure S8b)**, which will greatly influence the stability and current density especially at high overpotential.

Tafel slope was obtained from LSV curve by the Tafel equation ($\eta = a + b\log j$, η is overpotential, j is current density and b is the Tafel slope) to evaluate the kinetics of catalyst[50]. Apparently, $Co_3O_4/Fe_{0.33}Co_{0.66}P$ interface nanowire possesses the smallest Tafel slope, 59.8 mV dec^{-1}, further demonstrating the superiority of $Co_3O_4/Fe_{0.33}Co_{0.66}P$ at high current density, but that of RuO_2 on NF is as large as 156.6 mV dec^{-1}. And the Tafel slope of $Co_3O_4/Fe_{0.33}Co_{0.66}P$ is also smaller than those of Co-CHH/$FeCo_2(CN)_6$ (97.9 mV dec^{-1}), Co-CHH (82.6 mV dec^{-1}) and bare NF (104.6 mV dec^{-1}) **(see Figure 3c and Table S2)**.

Electrochemical impedance spectra (EIS) and electrochemical surface area (ECSA) were used to better understand the superior OER activity of $Co_3O_4/Fe_{0.33}Co_{0.66}P$ interface nanowire. It can be seen from **Figure 3d** that the impedance of the catalysts increases in the order of $Co_3O_4/Fe_{0.33}Co_{0.66}P$, RuO_2, Co-CHH/$FeCo_2(CN)_6$, Co-CHH and NF, consistent with the OER result. ECSA was used to evaluate the active surface area of catalyst **(Figure 3e and 3f)**. The ECSA value of $Co_3O_4/Fe_{0.33}Co_{0.66}P$ (8.69 mF cm^{-2}) is much larger than those of Co-CHH (2.92 mF cm^{-2}) and Co-CHH/$FeCo_2(CN)_6$ (3.78 mF cm^{-2}), indicating more exposure of active sites and better OER activity.

A series of control experiments are added to clarify our work. Firstly, we investigated the OER activity of catalysts generated under 0 h, 3 h and 18 h in second hydrothermal reaction. The overpotential for $Co_3O_4/Fe_{0.33}Co_{0.66}$ to reach the current density of 20 mA cm^{-2} is 99 mV, 102 mV and 151 mV smaller than those of CoP, Co_3O_4/FeP and $Fe_{0.33}Co_{0.66}P$, further indicating the significance of the second hydrothermal reaction and Co_3O_4/ $Fe_{0.33}Co_{0.66}P$ interface on boosting OER activity (Figure S9). Secondly, $Co_3O_4/FeCo_2O_4$ obtained by calcining Co-CHH/$FeCo_2(CN)_6$ without $NaH_2PO_2{\cdot}H_2O$ powder under the protection of Ar needs the overpotential of 255 mV to reach 20 mA cm^{-2} (Figure S9), suggesting the importance of phosphorization to OER activity of the electrocatalyst.

Furthermore, the catalyst prepared with the same procedure of Co_3O_4/ $Fe_{0.33}Co_{0.66}P$ except for the presence of NF was surveyed. Neither the morphology nor the OER performance (Figure S10) is superior to Co_3O_4/ $Fe_{0.33}Co_{0.66}P$, implying the significance of NF on guiding the formation of the Co_3O_4/ $Fe_{0.33}Co_{0.66}P$ nanointerface and enhancing OER activity. We also discussed the role of NF from the point of theoretical calculation later.

Stability is an indispensable feature to be reckoned with for an excellent catalyst. The electrochemical aging test was proceeded with 3000 cyclic voltammetry (CV) cycles. It can be seen from **Figure 4a** that OER performance for Co_3O_4/$Fe_{0.33}Co_{0.66}P$ from LSV curve acquired after 3000 cycles increased slightly instead of attenuation, demonstrating the superior stability. On the other hand, the long-time stability test was carried out at the overpotentials of 200 mV and 240 mV, respectively **(Figure 4b)**. The current-time curve at 200 mV was smoother than that at 240 mV because of the relative low current density (~ 30 mA cm^{-2}) at 200 mV. The current density loss under both overpotentials can be negligible even after 150 h. In addition, there are almost no crystalline structure **(Figure 4c)** and morphology changes (**Figure 4d-4f**) after 150 h under the overpotential of 200 mV, further suggesting the excellent stability of Co_3O_4/$Fe_{0.33}Co_{0.66}P$ interface nanowire.

From the view on free energy pathways for the Co_3O_4/$Fe_{0.33}Co_{0.66}P$ system, the trend by the IF region overall shows an energetic favorable process of water oxidation with a change of ΔG = 4.21 eV **(Figure 5a)**. The potential determining step (PDS) occurs at the splitting of hydroxyl group towards to adsorbed O* and the proton for these three different systems. The barriers are 4.63 eV, 3.40 eV, and 2.81 eV for the $Fe_{0.33}Co_{0.66}P$, Co_3O_4 and IF parts, respectively. We note that the first step of splitting H_2O into H + OH is actually energetically rather favorable at the IF region and gains the energy of -0.25 eV, compared to the 0.51 eV and 0.74 eV for the $Fe_{0.33}Co_{0.66}P$ and Co_3O_4 respectively. Regarding the H-chemisorption, we found the native CoP system has the chemisorption energy deep at ΔG = -0.60 eV which is usually over-binding, while $Fe_{0.33}Co_{0.66}P$ improves this issue and levels up to ΔG = -0.33 eV. The IF system ultimately favors in the H-desorption process as it

shows ΔG = 0.10 eV slightly higher than the thermoneutral line (ΔG = 0 eV), potentially indicating a favorable recovery of Co-oxidation state *via* desorption of H_2 by $2H \rightarrow H_2$ based on the H that chemically adsorbed at step of O_2 + 4H **(Figure 5b)**.

Local view on the atomic structural evolution confirms that H_2O can stabilize at the Co-site of the IF region because of the strong *p-d* overlapping effect. The intermediate species can be also stably located. Especially, the *OOH is stabilized by two Co-sites, and both Co and O sites can be active to locate the H^+ for further electron transfer within such electron-rich area **(Figure 5c)**. Actually, the $Co_3O_4/Fe_{0.33}Co_{0.66}P$-NF interface can be seen as a semi-metallic heterojunction and DFT study shows that the interface region is the electron-hole rich area which can be achieved by the highly efficient charge spatial separation and agglomeration. We finally study the electrochemical effects by the oxidation rate at the IF region and the Ni foam **(Figure S11-S15)** by discussing the physicochemical trends. We confirm the interface system not only contributes high electron current density of the system, but also lowers down overall energetic barrier for each step of the water oxidation process.

Conclusions

In summary, we demonstrate a new method for the fabrication of $Co_3O_4/Fe_{0.33}Co_{0.66}P$ interface nanowire for boosting oxygen evolution catalysis at high current density by partially chemical etching of Co-CHH with $Fe(CN)_6^{3-}$, followed by low temperature phosphorization with $NaH_2PO_2 \cdot H_2O$. The obtained $Co_3O_4/Fe_{0.33}Co_{0.66}P$ interface nanowire exerts awesome OER activity in 1.0 M KOH with the overpotential of 170 mV to reach the current density of 20 mA cm^{-2} and the Tafel slope of 59.8 mV dec^{-1}, which is caused by lower electrochemical catalytic barrier by the active Co and O sites from the $Co_3O_4/Fe_{0.33}Co_{0.66}P$ interface, proved by theoretical calculations. In particular, $Co_3O_4/Fe_{0.33}Co_{0.66}P$-NF has great advantage in enhancing OER catalysis at high current density, showing the overpotential of merely 291 mV at 800 mA cm^{-2}. Moreover, long-time stability test was carried out under the overpotentials of 200 mV and 240 mV for 150 hours. It turns out that

not only negligible current density loss is observed but also the crystal structure and morphology are well kept, manifesting the fantastic durability. This work opens a new avenue for the construction of interface nanomaterials and shed light on the relationship between the interface and OER activity.

Supporting Information

Supporting Information is available from the Wiley Online Library or from the author.

Acknowledgements

This study was financially supported by the National Natural Science Foundation of China (Grant No. 21427811), MOST, China (No. 2016YFA0203200 and 2016YFA0201300), Youth Innovation Promotion Association CAS (No. 2016208), Jilin province science and technology development plan project 20170101194JC, the National Natural Science Foundation of China (No.51671003), the National Basic Research Program of China (No. 2017YFA0206701), the start-up supports from Peking University and Young Thousand Talented Program and the China Postdoctoral Science Foundation (No. 2017M610018).

Received: ((will be filled in by the editorial staff))

Revised: ((will be filled in by the editorial staff))

Published online: ((will be filled in by the editorial staff))

References

[1] B. Zhang, X. Zheng, O. Voznyy, R. Comin, M. Bajdich, M. García-Melchor, L. Han, J. Xu, M. Liu, L. Zheng, F. P. García deArquer, C. T. Dinh, F. Fan, M. Yuan, E. Yassitepe, N. Chen, T.

Regier, P. Liu, Y. Li, P. De Luna, A. Janmohamed, H. L. Xin, H. Yang, A. Vojvodic, E. H. Sargent, *Science* 2016, *352*, 333.

[2] S. Yagi, I. Yamada, H. Tsukasaki, A. Seno, M. Murakami, H. Fujii, H. Chen, N. Umezawa, H. Abe, N. Nishiyama, *Nat. Commun.* 2015, *6*, 8249.

[3] Z. W. Seh, J. Kibsgaard, C. F. Dickens, I. Chorkendorff, J. K. Norskov, T. F. Jaramillo, *Science* 2017, *355*, 4998.

[4] Y. Jia, L. Z. Zhang, G. P. Gao, H. Chen, B. Wang, J. Z. Zhou, M. T. Soo, M. Hong, X. C. Yan, G. R. Qian, J. Zou, A. J. Du, X. D. Yao, *Adv. Mater.* 2017, *29*, 1700017.

[5] H. Shin, H. Xiao, W. A. Goddard, *J. Am. Chem. Soc.* 2018, DOI: 10.1021/jacs.8b02225.

[6] D. Zhao, Y. Pi, Q. Shao, Y. Feng, Y. Zhang, X. Huang, *ACS Nano* 2018, DOI: 10.1021/acsnano.8b03141

[7] M. W. Kanan, D. G. Nocera, *Science* 2008, *321*, 1072.

[8] H. Kim, J. Park, I. Park, K. Jin, S. E. Jerng, S. H. Kim, K. T. Nam, K. Kang, *Nat. Commun.* 2015, *6*, 8253.

[9] X. Fan, Y. Liu, S. Chen, J. Shi, J. Wang, A. Fan, W. Zan, S. Li, W. A. Goddard, X. M. Zhang, *Nat. Commun.* 2018, *9*, 1809.

[10] Y. Jia, L. Zhang, A. Du, G. Gao, J. Chen, X. Yan, C. L. Brown, X. Yao, *Adv. Mater.* 2016, *28*, 9532.

[11] Y. Jia, J. Chen, X. Yao, *Mater. Chem. Front.* 2018, *2*, 1250

[12] L. Zhang, Y. Jia, G. Gao, X. Yan, N. Chen, J. Chen, M. T. Soo, B. Wood, D. Yang, A. Du, X. Yao, *Chem* 2018, *4*, 285.

[13] A. L. Strickler, M. A. Escudero-Escribano, T. F. Jaramillo, *Nano Lett.* 2017, *17* , 6040.

[14] Y. Tang, H. J. Xu, J. Cao, C. F. Shan, B. K. Wang, P. X. Xi, W. S. Liu, *Angew. Chem. Int. Ed.* 2018, DOI: 10.1002/anie.201804673.

[15] B. S. Yeo, A. T. Bell, *J. Am. Chem. Soc.* 2011, *133*, 5587.

[16] W. Lu, T. Liu, L. Xie, C. Tang, D. Liu,, S. Hao, F. Qu, G. Du, Y. Ma, A. M. Asiri, X. Sun, *Small* 2017, *13*, *1700805.*

[17] J. Zhou, Y. Dou, A. Zhou, R.-M. Guo, M.-J. Zhao, J.-R. Li, *Adv. Energy Mater.* 2017, *7*, 1602643.

[18] Z. Fang, L. Peng, H. Lv, Y. Zhu, C. Yan, S. Wang, P. Kalyani, X. Wu, G. Yu, *ACS Nano* 2017, *11*, 9550.

[19] Y. Pan, K. Sun, S. Liu, X. Cao, K. Wu, W. C. Cheong, Z. Chen, Y. Wang, Y. Li, Y. Liu, D. Wang, Q. Peng, C. Chen, Y. Li, *J. Am. Chem. Soc.* 2018, *140*, 2610.

[20] X. Han, G. He, Y. He, J. Zhang, X. Zheng, L. Li, C. Zhong, W. Hu, Y. Deng, T.-Y. Ma, *Adv. Energy Mater.* 2018, *8*, 1702222.

[21] S.-F. Hung, Y.-Y. Hsu, C.-J. Chang, C.-S. Hsu, N.-T. Suen, T.-S. Chan, H. M.Chen, *Adv. Energy Mater.* 2018, *8*, 1701686.

[22] Z. Wang, H. Liu, R. Ge, X. Ren, J. Ren, D. Yang, L. Zhang, X. Sun, *ACS Catal.* 2018, *8*, 2236.

[23] A. Aijaz, J. Masa, C. Rosler, W. Xia, P. Weide, A. J. Botz, R. A. Fischer, W.Schuhmann, M. Muhler, *Angew. Chem. Int. Ed.* 2016, *55*, 4087.

[24] Y. Liang, Y. Li, H. Wang, J. Zhou, J. Wang, T. Regier, H. Dai, *Nat. Mater.* 2011, *10*, 780.

[25] J. Wang, F. Ciucci, *Small* 2017, *13*, 1604103.

[26] H. Hu, B. Guan, B. Xia, X. W. Lou, *J. Am. Chem. Soc.* 2015, *137*, 5590.

[27] T. W. Kim, M. A. Woo, M. Regis, K. S. Choi, *J. Phys. Chem. Lett.* 2014, *5*, 2370.

[28] Y. Sun, T. Zhang, X. Li, D. Liu, G. Liu, X. Zhang, X. Lyu, W. Cai, Y. Li, *Chem. Commun.* 2017, *53*, 13237.

[29] H.-C. Li, Y.-J. Zhang, X. Hu, W.-J. Liu, J.-J. Chen, H.-Q. Yu, *Adv. Energy Mater.* 2018, *8*, 1702734.

[30] G.-P. Kim, H.-H. Sun, A. Manthiram, *Nano Energy* 2016, *30*, 130.

[31] J. Yin, Y. Li, F. Lv, Q. Fan, Y. Q. Zhao, Q. Zhang, W. Wang, F. Cheng, P. Xi, S. Guo, *ACS Nano* 2017, *11*, 2275.

[32] J. Yin, Y. Li, F. Lv, M. Lu, K. Sun, W. Wang, L. Wang, F. Cheng, Y. Li, P. Xi, S. Guo, *Adv. Mater.* 2017, *29*,1704681.

[33] L. An, Y. Li, M. Luo, J. Yin, Y.-Q. Zhao, C. Xu, F. Cheng, Y. Yang, P. Xi, S. Guo, *Adv. Funct. Mater*. 2017, *27*, 1703779.

[34] R. Zhang, G. Wen, H. Adidharma, A. G. Russell, B. Wang, M. Radosz, M. Fan, *ACS Catal.* 2017, *7*, 8285.

[35] K. Liu, C. Zhang, Y. Sun, G. Zhang, X. Shen, F. Zou, H. Zhang, Z. Wu, E. C. Wegener, C. J. Taubert, J. T. Miller, Z. Peng, Y. Zhu, *ACS Nano* 2018, *12*, 158.

[36] C. Tang, L. Gan, R. Zhang, W. Lu, X. Jiang, A. M. Asiri, X. Sun, J. Wang, L. Chen, *Nano Lett.* 2016, *16*, 6617.

[37] M. Garcia-Mota, M. Bajdich, V. Viswanathan, A. Vojvodic, A. T. Bell, J. K. Nørskov, *J. Phys. Chem. C* 2012, *116*, 21077

[38] J. D. Blakemore, H. B. Gray, J. R. Winkler, A. M. Müller, *ACS Catal.* 2013, *3*, 2497.

[39] H. S. Ahn, A. J. Bard, *J. Am. Chem. Soc.* 2015, *137*, 612

[40] I. Roger, M. D. Symes, *J. Am. Chem. Soc.* 2015, 137, *43*, 13980.

[41] H. Kim, J. Park, I. Park, K. Jin, S. E. Jerng, S. H. Kim, K. T. Nam, K. Kang, *Nat. Commun.* 2015, *6*, 8253.

[42] L. Cui, F. Qu, J. Liu, G. Du, A. M. Asiri, X. Sun, *ChemSusChem* 2017, *10*, 1370.

[43] E. Edri, J. K. Cooper, I. D. Sharp, D. M. Guldi, H. Frei, *J. Am. Chem. Soc*. 2017, *139*, 5458.

[44] X. Zhang, Y. Chen, P. V. Kamat, S. Ptasinska, *J. Phys. Chem. C* 2018, *122*, 13894.

[45] X. Ji, R. Zhang, X. Shi, A. M. Asiri, B. Zheng, X. Sun, *Nanoscale*, 2018, *10*, 7941

[46] H. Wan, R. Ma, X. Liu, J. Pan, H. Wang, S. Liang, G. Qiu, T. Sasaki, *ACS Energy Lett*. 2018, *3*, 1254.

[47] B. Huang, *Phys. Chem. Chem. Phys.* 2017, *19*, 8008.

[48] B. Huang, *J. Comput. Chem.* 2016, *37*, 825.

[49] C. Tang, N. Cheng, Z. Pu, W. Xing, X. Sun, *Angew. Chem., Int. Ed.* 2015, *54*, 9351.

[50] L. Yu, J. F. Yang, B. Y. Guan, Y. Lu, X. W. Lou, *Angew. Chem. Int. Ed.* 2018, *57*, 172.

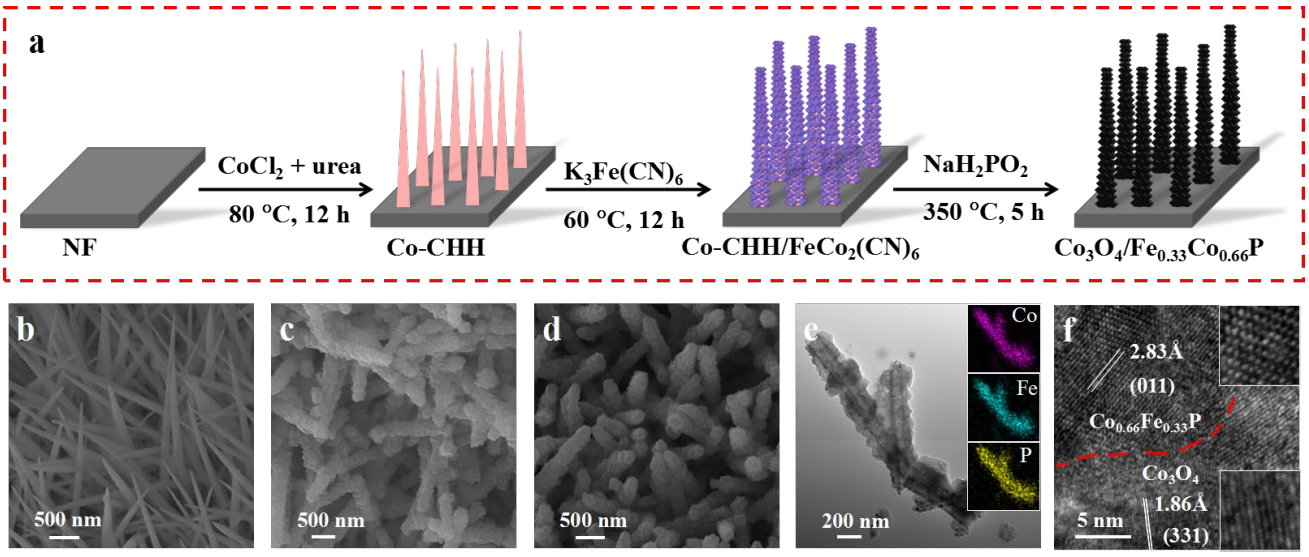

Figure 1. (a) Schematic illustration of the synthesis of $Co_3O_4/Fe_{0.33}Co_{0.66}P$ interface nanowire. SEM images of (b) Co-CHH, (c) Co-CHH/$FeCo_2(CN)_6$ and (d) $Co_3O_4/Fe_{0.33}Co_{0.66}P$. (e) TEM and (f) HRTEM images of $Co_3O_4/Fe_{0.33}Co_{0.66}P$ interface nanowire. *Inset* in (e): elemental mapping images of Co, Fe and P.

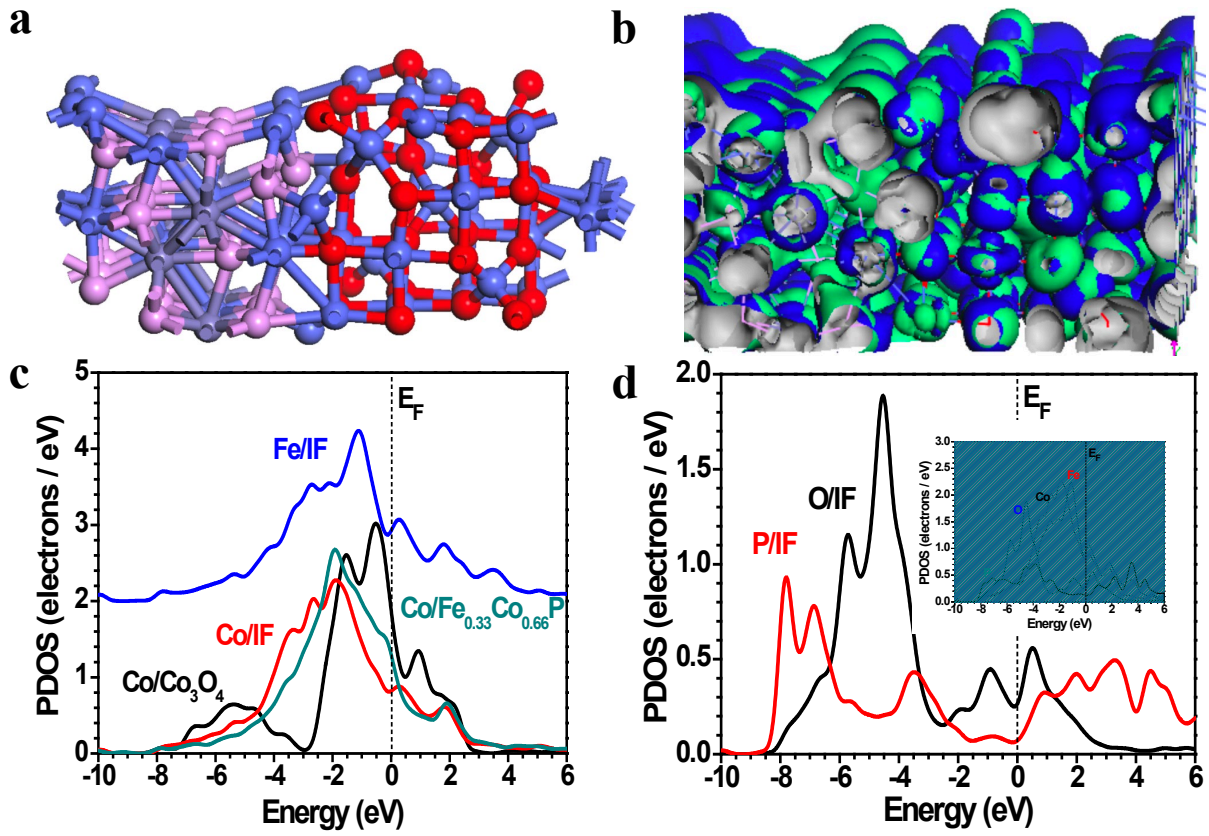

Figure 2. (a) The local atomic structure of the interface system built by the Co_3O_4 and $Co_{0.66}Fe_{0.33}P$ parts. (b) Local orbital 3D contour plots of the HOMO and LUMO near the E_F. (c) The PDOSs of the Co-3d-bands from different regions within the IF system. (d) The PDOSs of the P-3p and O-2p bands at the IF region and the different orbital overlapping effects (insertion).

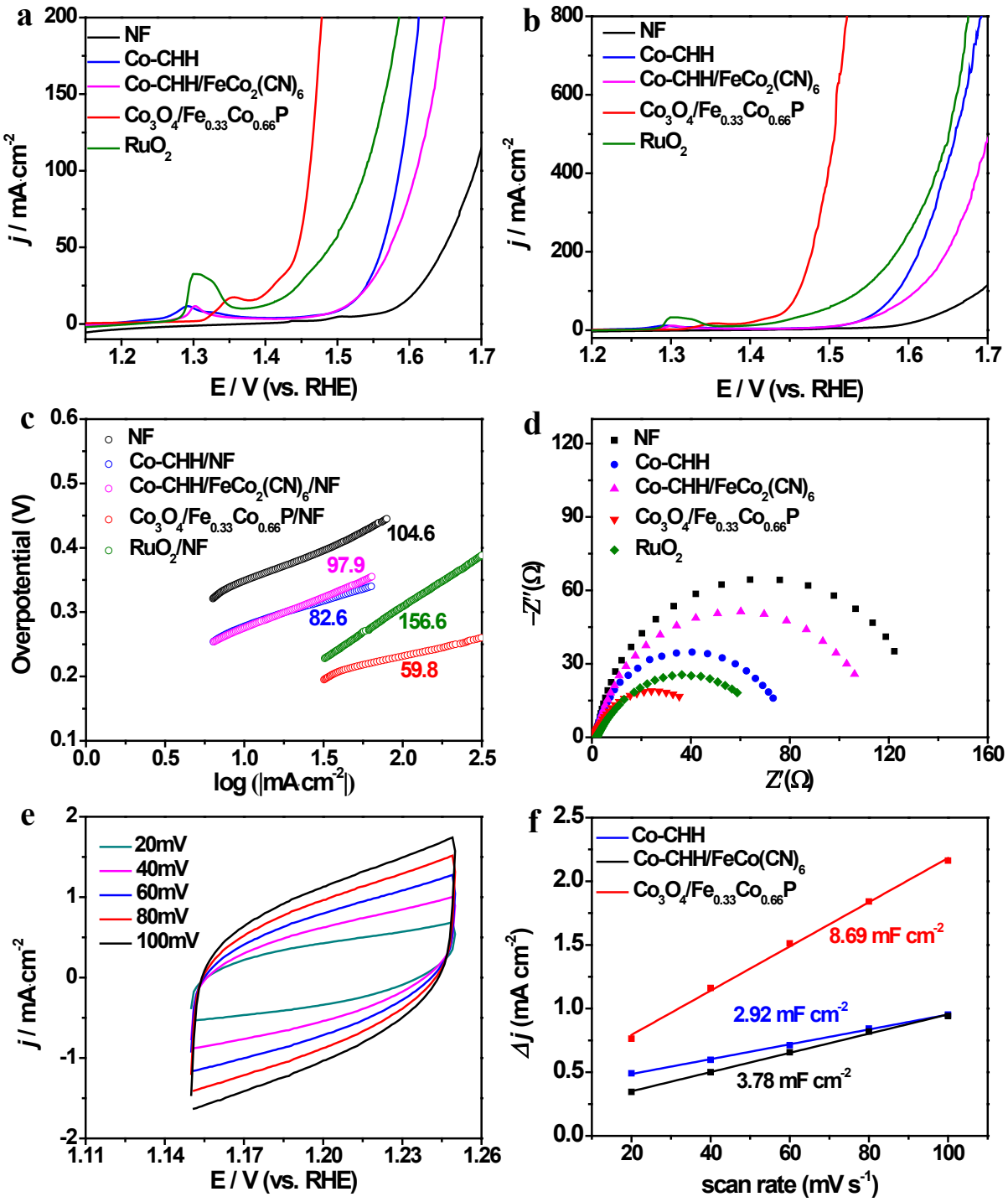
a
NF
Co-CHH
Co-CHH/FeCo2(CN)6
Co3O4/Fe0.33Co0.66P
RuO2
j / mA·cm-2
E / V (vs. RHE)
b
NF
Co-CHH
Co-CHH/FeCo2(CN)6
Co3O4/Fe0.33Co0.66P
RuO2
j / mA·cm-2
E / V (vs. RHE)
c
NF
Co-CHH/NF
Co-CHH/FeCo2(CN)6/NF
Co3O4/Fe0.33Co0.66P/NF
RuO2/NF
104.6
97.9
82.6
156.6
59.8
Overpotential (V)
log (|mA·cm-2|)
d
NF
Co-CHH
Co-CHH/FeCo2(CN)6
Co3O4/Fe0.33Co0.66P
RuO2
-Z''(Ω)
Z'(Ω)
e
20mV
40mV
60mV
80mV
100mV
j / mA·cm-2
E / V (vs. RHE)
f
Co-CHH
Co-CHH/FeCo(CN)6
Co3O4/Fe0.33Co0.66P
8.69 mF cm-2
2.92 mF cm-2
3.78 mF cm-2
Δj (mA cm-2)
scan rate (mV s-1)

Figure 3. (a,b) Polarization curves and (c) Tafel plots of NF, Co-CHH, Co-CHH/$FeCo_2(CN)_6$, $Co_3O_4/Fe_{0.33}Co_{0.66}P$ and RuO_2 for OER in 1.0 M KOH. (d) EIS of NF, Co-CHH, Co-CHH/$FeCo_2(CN)_6$, $Co_3O_4/Fe_{0.33}Co_{0.66}P$ and RuO_2. (e) Cyclic voltammetry curves for $Co_3O_4/Fe_{0.33}Co_{0.66}P$ at different scan rates. (f) C_{dl} for Co-CHH, Co-CHH/$FeCo_2(CN)_6$ and $Co_3O_4/Fe_{0.33}Co_{0.66}P$ obtained at 1.2 V (*vs.* RHE).

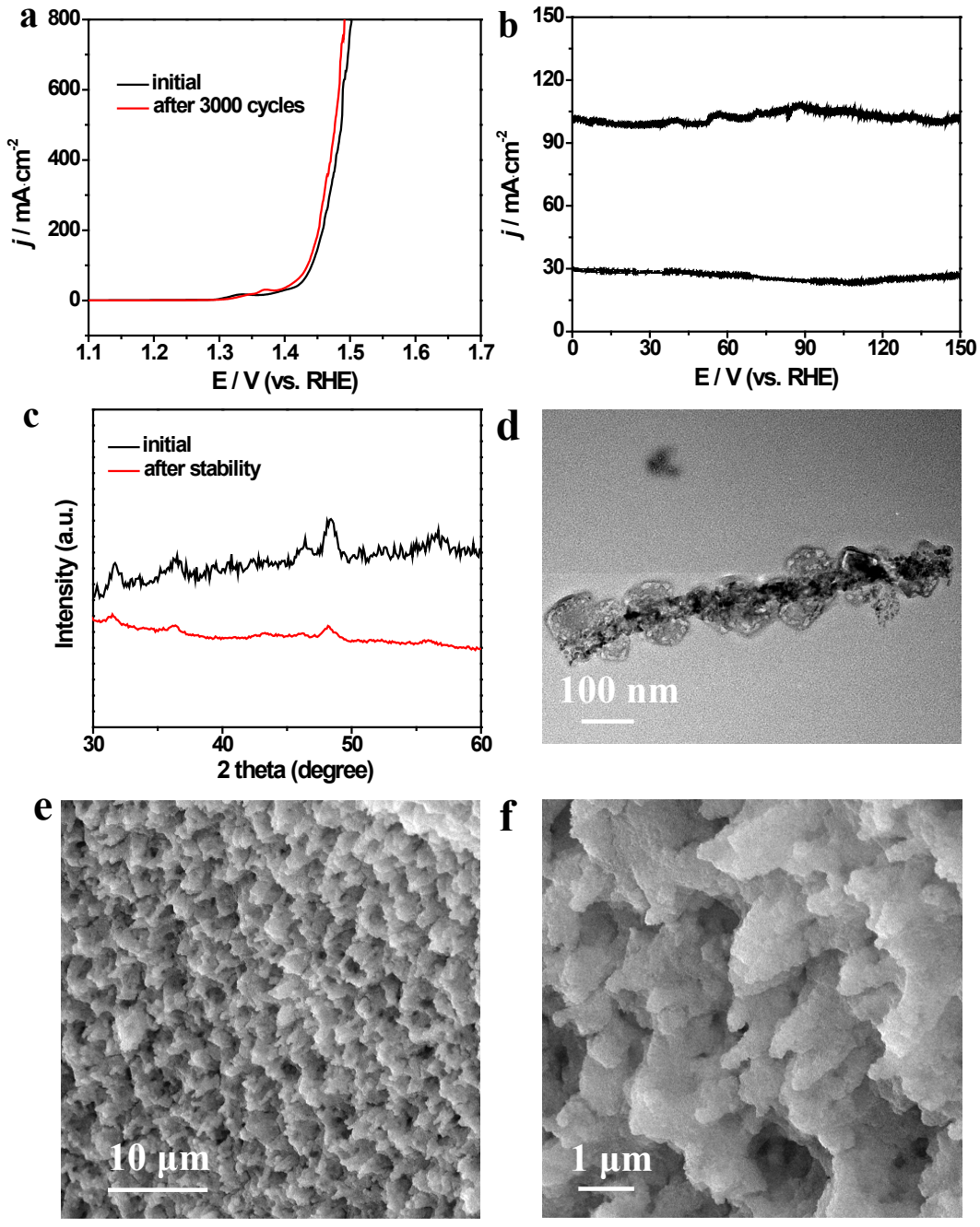

Figure 4. (a) LSV curves of $Co_3O_4/Fe_{0.33}Co_{0.66}P$ on NF before and after 3000 cyclic voltammetry cycles between 1.1 V and 1.5 V vs RHE. (b) Time-dependent current density curve of $Co_3O_4/Fe_{0.33}Co_{0.66}P$ on NF under constant overpotential of 200 mV and 240 mV for 150 hours. (c) XRD pattern (d) TEM image, (e-f) SEM images of $Co_3O_4/Fe_{0.33}Co_{0.66}P$ on NF before and after 150 h stability test.

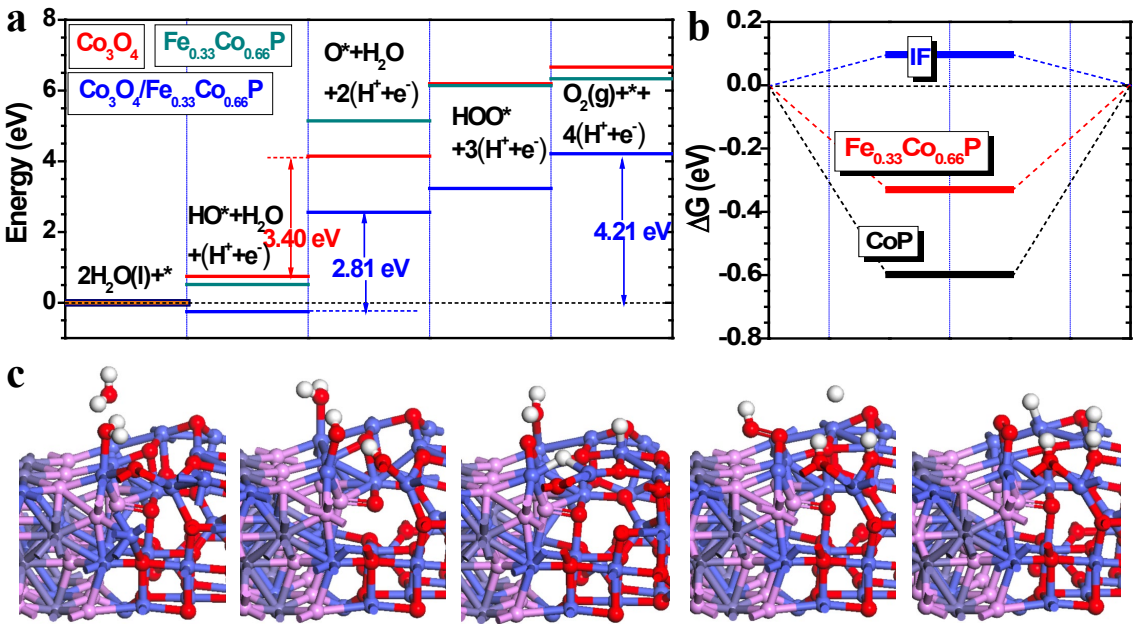

Figure 5. (a) The free energetic pathway of water oxidation of the three different parts of such interface system. (b) The chemisorption energy of H on the surfaces of CoP, Fe-doped CoP and IF, respectively. (c) Local atomic structural evolution of the water oxidation at the IF region.

A universal strategy for the fabrication of $Co_3O_4/Fe_{0.33}Co_{0.66}P$ interface nanowire is rationally designed and synthesized by partially chemical etching $Co(CO_3)_{0.5}(OH)\cdot 0.11H_2O$ nanowire with $Fe(CN)_6^{3-}$, followed by low temperature phosphorization with $NaH_2PO_2\cdot H_2O$ for boosting oxygen evolution.

Xiaoyan Zhang, Jing Li*, Yong Yang, Shan Zhang, Haishuang Zhu, Xiaoqing Zhu, Huanhuan Xing, Bolong Huang*, Shaojun Guo* and Erkang Wang

Nanowire; Semi-metallic interface; Oxygen evolution reaction; Electrocatalysis

Title: $Co_3O_4/Fe_{0.33}Co_{0.66}P$ Interface Nanowire for Enhancing Water Oxidation Catalysis at High Current Density

TOC figure